Applied Surface Science 355 (2015) 1161–1167

Contents lists available at ScienceDirect

Applied Surface Science

journal homepage: www.elsevier.com/locate/apsusc

Surface chemistry and reactivity of SiO_2 polymorphs: A comparative study on α-quartz and α-cristobalite

Cuihua Tang[a,b,c], Jianxi Zhu[a,b,*], Zhaohui Li[d,**], Runliang Zhu[a,b], Qing Zhou[a,b,c], Jingming Wei[a,b], Hongping He[a,b], Qi Tao[a,b]

[a] CAS Key Laboratory of Mineralogy and Metallogeny, Guangzhou Institute of Geochemistry, Chinese Academy of Sciences, 511 Kehua Street, Guangzhou 510640, China
[b] Guangdong Provincial Key Laboratory of Mineral Physics and Materials, 511 Kehua Street, Guangzhou 510640, China
[c] University of Chinese Academy of Sciences, 19 Yuquan Road, Beijing 100049, China
[d] Geosciences Department, University of Wisconsin – Parkside, Kenosha, WI 53141, USA

ARTICLE INFO

Article history:
Received 10 June 2015
Received in revised form 30 July 2015
Accepted 30 July 2015
Available online 4 August 2015

Keywords:
Surface reactivity
Silica polymorphs
α-Quartz
α-Cristobalite
Adsorption
Methylene blue

ABSTRACT

Silica minerals are widely used in environmental remediation for their prevalence in soil and sediment. Two common SiO_2 polymorphs, α-quartz and α-cristobalite, were investigated for the removal of a typical cationic dye, methylene blue (MB), from aqueous solutions. Their adsorption behaviors were studied in batch experiments as a function of specific surface area (SSA), pH, and temperature. The surface site density of α-quartz (10.6 sites/nm^2) was higher than that of α-cristobalite (6.2 sites/nm^2) with the Gran plot method, and the adsorption maxima of MB on the two were 0.84 mg/m^2 and 0.49 mg/m^2, respectively, at 303 K and pH 8. The potentiometric titration showed the capacity of proton-donating by α-quartz was stronger than that by α-cristobalite. A drastic increase of adsorption amount on α-quartz at pH < 3 was caused by its greater quantity of isolated silanols. The negative ΔG and positive ΔH values suggested adsorption of MB on both minerals was spontaneous and endothermic. At three different temperatures (288 K, 298 K, and 303 K), the adsorption capacities of two polymorphs increased with increasing temperature. The surface heterogeneity of α-quartz and α-cristobalite corresponds to their different adsorption behavior, and our work also provides some referential significance in evaluating the overall quality of soils and sediments.

1. Introduction

Silica minerals, whose abundance in the earth's crust is as high as 12%, not only are extensively present in rocks, soils, sediments, and dustfalls, but also dominate many geochemistry processes, as well as physical, chemical and biological characteristics of subsurface environments [1–5]. The adsorption of charged species at the silica–water interface is an important process in understanding environmental sinks, both terrestrial and aquatic, of a number of organics and heavy metal ions [6]. Dyes are well known to be used in many industries such as textiles, pulpmills, leather, dye synthesis, printing, food, and plastics, which comprise the major source of colored effluents [7]. Most of the effluents could be not only just hazardous for the environment, but also toxic for human beings [8,9]. As the most abundant minerals in the soils and sediments, silica minerals play irreplaceable roles in the fate of these dye pollutants. Meanwhile, the interface reaction between silica minerals and the dyes exerts a substantial effect in the environmental process of soils and sediments.

The diversity of the SiO_4 tetrahedron polymerization style results in various SiO_2 polymorphs with different crystal structures [10]. Crystalline silica occurs with some common polymorphs, such as quartz, cristobalite, and tridymite. Specifically, α-quartz is the most general mineral in the continental crust and is the most commonly encountered polymorph, and α-cristobalite usually occurs in the dustfalls of the ceramics industry [11]. In the crystal structures, silicon and oxygen bond with different bond lengths and bond angles always break in a random pattern. The different atomic arrangement and various forms of Si—O bond cleavage in the crystal structures of α-quartz and α-cristobalite lead to their difference in surface microstructure, which dominates the quite different surface properties of these polymorphs [12,13]. To a large extent, the structural and chemical characteristics of the surface functional

* Corresponding author at: CAS Key Laboratory of Mineralogy and Metallogeny, Guangzhou Institute of Geochemistry, Chinese Academy of Sciences, 511 Kehua Street, Guangzhou 510640, China.
** Corresponding author.
E-mail address: zhujx@gig.ac.cn (J. Zhu).

http://dx.doi.org/10.1016/j.apsusc.2015.07.214
0169-4332/

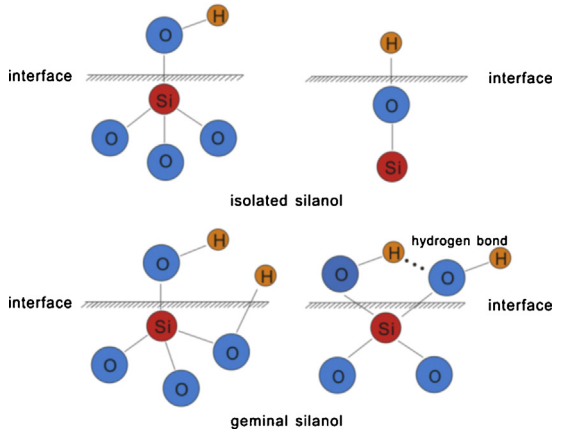

Fig. 1. Different species of surface silanols exhibited on the silica surface.

groups perform a crucial role in the physical–chemical processes at the mineral–environment interface [14].

Nuclear magnetic resonance (NMR) studies have revealed that the silica surface contains two types of surface functional groups: silanols (Si—OH) known as Q^2 and Q^3 [15,16], which determine its surface chemistry and reactivity. The Q^2 site has two Si—OH groups pointing away from the surface with two Si—O groups pointing into the bulk (O_2—Si—$(OH)_2$), whereas the Q^3 site has the structure O_3—Si—OH, which is clearly depicted in Fig. 1 Previous computational reports showed that heterogeneity of silanol species and its distribution occur not only on different dominant crystal planes but also in different silica polymorphs. Murashov et al. [14] considered that the average silanol density in a fractured particulate of α-quartz was larger than that of α-cristobalite. Meanwhile, the proportion of isolated silanols in both α-quartz and α-cristobalite was larger than that of germinal silanols. Musso et al. [17] discussed the distribution and density of surface hydroxyl groups on different crystallographic planes with periodic B3LYP calculations, as well as H-bond interactions and their spectral signatures. They thought the thermodynamics of surface hydroxylation correlated with the strength of the H-bonds formed at the surfaces, as measured by the bathochromic shift of the ν (OH) stretching frequency with respect to the value for a free surface OH group. However, the ideal molecular simulation results still lack support with adequate experimental evidences, and the different behaviors of the two silanols are not yet very clear. To investigate the heterogeneity of the surface microstructure and properties of some SiO_2 polymorphs, Fubini and his colleagues used water and alcohols as probe molecules to measure the adsorption enthalpy and test the hydrophilicity/hydrophobicity [18–21]. Although some studies on the interface reactions of SiO_2 polymorphs have been conducted, they focused merely on the interaction between the SiO_2 polymorphs and some small model molecules (e.g., water, ammonia, and alcohols) in a relatively simple environment. In fact, the interactions between silica polymorphs and charged species are very different from the reactions via hydrogen bonds only. Therefore, detailed information on the interface reactions with charged species will provide a much more comprehensive understanding of the surface heterogeneity of some SiO_2 polymorphs and their significant importance in environmental remediation.

The primary purpose of this work was to elucidate the heterogeneity of two common SiO_2 polymorph minerals, α-quartz and α-cristobalite, in the adsorption of methylene blue (MB) from aqueous solutions. First, the surface site density and potentiometric distribution were measured directly by the method of Gran plots and zeta potential titration, respectively. Then, we investigated the effect of the specific surface area (SSA), pH and temperature on the adsorption capacities of MB on α-quartz and α-cristobalite from aqueous solutions by batch adsorption experiments. Meanwhile, their different adsorption behaviors in response to various factors were also discussed in detail. According to our research, a better understanding of the surface microstructure and property of SiO_2 polymorphs will exert a great guiding significance in mineral–environment interface processes and industrial applications. Hence, it should take their surface heterogeneity into consideration while evaluating the environmental behaviors of SiO_2 minerals system.

2. Materials and methods

2.1. Materials

The α-quartz sample was naturally collected from Guiding County, Guizhou Province of China, and the commercially available α-cristobalite sample was purchased from Veston Silicon Co., Ltd. (Guiping City, Guangxi Province of China). To obtain homogeneously finer powders, both samples were ground by a planetary ball grinder (FRITSCH Pulverisette 6, Germany) for 2 h. The powder samples were immersed in a 0.01 M HCl solution for 24 h and then rinsed with deionized water until they are free of chloride ions. After drying, the samples were calcined in a muffle furnace at 450 °C for 12 h to remove possible organics.

The reagent-grade MB ($C_{16}H_{18}N_3SCl{\cdot}3H_2O$, purity ≥ 98.5%) and crystal violet (CV) ($C_{25}H_{30}N_3Cl{\cdot}3H_2O$, purity ≥ 99.0%) were purchased from Tianjin Kemiou Chemical Reagent Co., Ltd and were used as received. The solutions were prepared with deionized water, and the pH was adjusted with standard acid solution (0.1 M HCl) and standard base solution (0.1 M NaOH).

2.2. Characterization

Powder X-ray diffraction (XRD) measurements were performed to confirm the structures of α-quartz and α-cristobalite, using a Bruker D8 ADVANCE X-ray diffractometer operated at 40 kV and 40 mA with Cu Kα radiation. The diffraction patterns were recorded at a scanning speed of 3°/min and at a 2θ range between 20° and 80°. The selected minerals were quantitatively analyzed with the reference intensity ratio (RIR) method.

Nitrogen adsorption/desorption isotherms were measured at −196 °C using a Micromeritics ASAP 2020M specific surface area and porosity analyzer. Before analysis, both samples were outgassed at 120 °C for 8 h. The SSA was calculated based on the Brunauder, Emmertt, Teller (BET) equation.

Fourier-transform infrared spectroscopy (FTIR) spectra of the samples were recorded on a Bruker Vertex-70 Fourier-transform infrared spectrometer. The specimens were prepared by thorough mixing 0.9 mg of the sample powder with 80 mg of KBr, and the mixture was pressed into a pellet. More than 64 scans were collected for each measurement at a resolution of 2 cm^{-1}.

2.3. Surface site titration

Acid–base titration experiments were conducted at ambient temperature (28 °C). In the experiments, 0.5 g of α-quartz and α-cristobalite powders were added to two conical flasks with 50 mL of deionized water, and the flasks were marked as A and B, respectively. One more conical flask marked as C was prepared for a blank experiment without any sample powder and with 50 mL of deionized water only. Two drops of 0.1 M NaCl solution were added to all three conical flasks as the electrolyte. Then, the suspensions were stirred on a magnetic stirring apparatus for 12 h at ambient temperature. After that, suspensions in flasks A, B, and C were titrated to a pH of approximately 1.8 with a standard HCl solution

(0.1071 mol/L). Then, a standard NaOH solution (0.1037 mol/L) was used to back-titrate the suspensions to a pH of approximately 10.6. The pH values were measured by a pH meter (PHS-3C, Shanghai LeiCi, China).

2.4. Zeta potential distribution measurement

The surface zeta potentials of α-quartz and α-cristobalite were measured using an automatic zeta potential analyzer (MPT-2/Zetasizer Nano ZS, Malvern Instruments Ltd., England). Briefly, 0.1 g of α-quartz and α-cristobalite powders were dispersed in 20 mL of 0.01 M KCl electrolyte solutions, and stirred on a magnetic stirring apparatus for 20 min. After standing for 5 min, 10 mL of the supernatant was used for potentiometric titration. The pH of the suspensions was adjusted to the desired value in the range of 1–9 with 0.05 M/0.1 M HCl solutions and 0.05 M NaOH solution.

2.5. Adsorption experiments

Adsorption experiments of α-quartz and α-cristobalite with different SSA were performed at ambient temperature and pH 7. α-Quartz and α-cristobalite (0.4 g) with different SSA and 20 mL of MB solution with an initial concentration of 30 mg/L were added to each 50 mL polypropylene centrifuge tube. The mixtures were shaken continuously at 160 rpm for 24 h in an incubator shaker at 28 ± 1 °C. Then, the samples were centrifuged at 4200 rpm for 10 min. The supernatant solutions were diluted to appropriate concentrations with deionized water and characterized using ultraviolet–visible spectrophotometer (PerkinElmer Lambda 850 UV/VIS Spectrometer, America) at a wavelength of 664 nm. The same experimental procedure was used for CV adsorption, and the UV–Vis detection wavenumber was set at 583 nm. For the initial pH experiments, the same experimental conditions mentioned before were followed, except that the initial MB concentration was 40 mg/L and the initial pH values were from 2 to 10. Adsorption isotherms were determined at pH values of 3, 5, and 8 with initial MB concentrations of 5, 10, 20, 30, 40, 50, 60, and 70 mg/L. For temperature dependent experiments, the pH was maintained at approximately 8 while the temperatures were at 288, 298, and 303 K.

3. Results and discussions

3.1. Characterization of α-quartz and α-cristobalite

Powder XRD patterns of α-quartz and α-cristobalite revealed no characteristic reflections of impurities, suggesting that both were of high purity [13]. The calculated results based on the RIR method indicated that the purity were higher than 95% for both minerals.

The characteristic structural vibrations in the FTIR spectra (Fig. 2) were studied, and three main vibration bands were classified: (1) Si—O bending vibration at 470 cm^{-1} and 515 cm^{-1} for α-quartz [22] and at 491 cm^{-1} as a singlet for α-cristobalite; (2) Si—O—Si symmetrical stretching vibration at 796 cm^{-1} for α-cristobalite and at 780 cm^{-1} and 799 cm^{-1} as a doublet for α-quartz, which are its characteristic vibrations; (3) Si—O—Si asymmetrical stretching vibration located at 1098 cm^{-1} for α-quartz and at a larger wavenumber (1106 cm^{-1}) for α-cristobalite. The different vibration wavenumbers were caused by the various bond lengths and bond angles in the structures of α-quartz and α-cristobalite.

3.2. In situ Gran plot method

When dissolution and precipitation reactions play a less dominant role at the solid–liquid interface, the concentration of free hydrogen ions in the solution is controlled by surface chemical

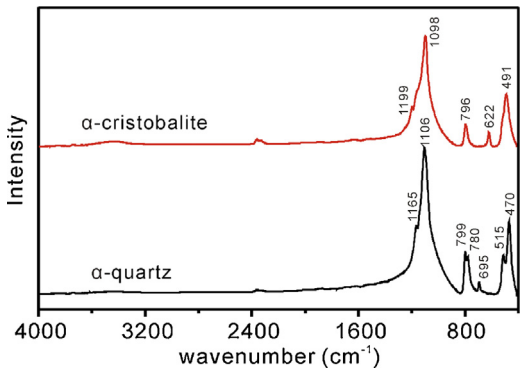

Fig. 2. FTIR spectra of α-quartz and α-cristobalite samples.

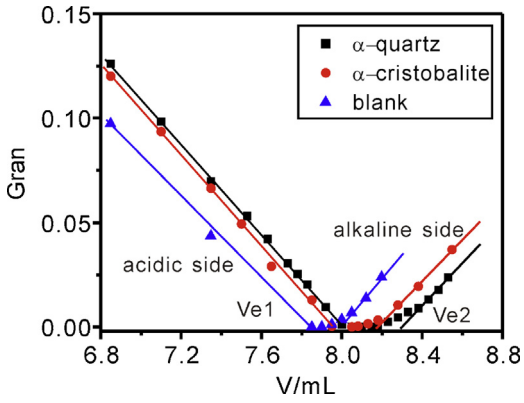

Fig. 3. Gran plots for α-quartz and α-cristobalite dispersions.

reactions. The in situ Gran plot method is commonly used to determine the total surface site concentration of oxides and silicate minerals in solutions [23,24]. The Gran function value of 10^{-pH} $(V_0 + V_a + V_b)$ (acidic side) or 10^{pH-14} $(V_0 + V_a + V_b)$ (alkaline side) was set as the *y*-coordinate, and the added hydroxyl volume was set as the *x*-coordinate. V_0, V_a, and V_b were the initial volume (mL) of the suspension, the volume of HCl added in the acid titration and the volume of NaOH added in the hydroxyl back-titration, respectively. During the hydroxyl back-titration, the added NaOH first reacted with the excess HCl added in the acid titration (reaction (1)). After that, the added OH^- began to react with silanols (Si—OH) on the solid surface (reaction (2)), and the remainder contributed to increasing the pH value of the system (reaction (3)). This result is clearly shown in the Gran plots (Fig. 3). The titration demarcation point of reaction (1) and reaction (2) was the *Ve*1 point, and the *Ve*2 point separated reaction (2) from reaction (3). From the plot, the *Ve*1 and *Ve*2 points of α-quartz and α-cristobalite were not identical owning to their different surface properties, which implied that they were equipped with different buffering capacities to hydroxyls [24,25]. Therefore, the concentration of surface sites (H_s, mol/L) of α-quartz and α-cristobalite could be calculated from the two equivalence points (*Ve*1 and *Ve*2) in the Gran plot of the hydroxyl titration after subtracting the hydroxyl consumed in the blank experiment, as shown in the equation below:

$$H_s = \frac{(Ve2_{sample} - Ve1_{sample})C_b - (Ve2_{blank} - Ve1_{blank})C_b}{V_0} \quad (1)$$

where C_b is the concentration of the NaOH solution (mol/L). Then, the surface site density (D_s, sites/nm^2) of α-quartz and α-cristobalite could be obtained from the following equation:

$$D_s = \frac{H_s N_A}{S C_s 10^{18}} \quad (2)$$

Table 1
Total surface site concentration (H_s) and surface site density (D_s) in α-quartz and α-cristobalite suspensions.

Sample	C_s (g/L)	H_s (10^{-4} mol/L)	D_s (sites/nm^2)
α-Quartz	10	2.90	10.6
α-Cristobalite	10	1.87	6.2

where N_A is the Avogadro constant (6.022×10^{23}), S is the BET SSA (m^2/g), and C_s is the solid concentration in the suspensions (g/L).

The total surface site density (D_S) of α-quartz was 10.6 sites/nm^2, which was higher than that of α-cristobalite (6.2 sites/nm^2) (Table 1). The results were similar to our previous data determined by traditional acid–base titration method [13]. Also, the result of α-quartz was in line with previous references by different measure methods, which reported the range of 5–12 sites/nm^2 [26,27]. While, all of our experimental results tended to be larger than the computational data [14] because of experimental deviation. As shown in the Gran plots, the higher surface site density in α-quartz corresponded to its higher buffering capacity to the hydroxyl solution, implying that α-quartz would behave quite differently in geochemical and environmental processes, compared with α-cristobalite.

3.3. Zeta potential measurement and potentiometric titration

The zeta potential distributions of α-quartz and α-cristobalite suspensions over a pH range of 1–9 are shown in Fig. 4 and the points of zero charge (pH_{PZC}) of the two minerals are given in Table 2. According to the figure, the pH_{PZC} of α-quartz was approximately 2.8, which was lower than that of α-cristobalite (3.2). As per the protonation and deprotonation reactions, the lower pH_{PZC} value indicated that α-quartz surface was more acidic than α-cristobalite [28]. In other words, the capacity of proton-donating by α-quartz was stronger than that by α-cristobalite.

The difference in the zeta potentials of the two SiO_2 polymorphs and their response to acid/alkali can be understood by taking into consideration the different crystal structures and dominant crystal orientations of α-quartz and α-cristobalite. Murashov et al. [14] determined that the (1 0 1) plane occurred with the highest

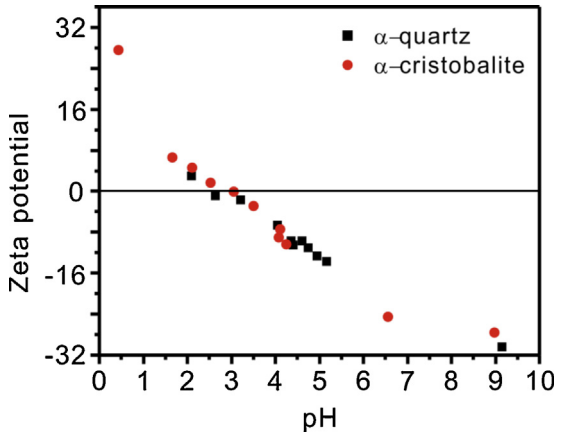

Fig. 4. Zeta potential as a function of pH for α-quartz and α-cristobalite in the presence of 0.01 M KCl.

Table 2
pH_{PZC} and the specific surface area of α-quartz and α-cristobalite.

Sample	pH_{PZC}	Specific surface area (m^2/g)
α-Quartz	2.8	1.66
α-Cristobalite	3.2	1.81

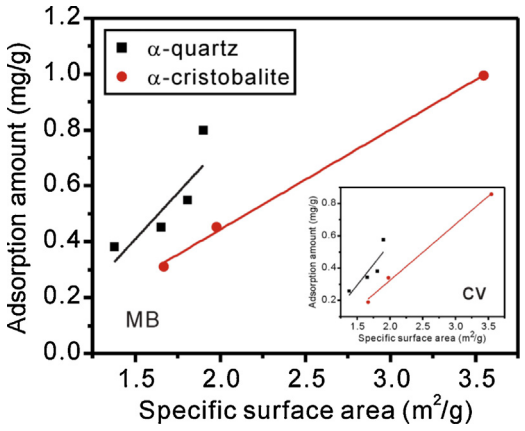

Fig. 5. The amount of adsorbed MB as a function of SSA of α-quartz and α-cristobalite.

probability in α-quartz and was 100% covered by isolated silanols, whereas the (0 0 1) plane was covered by 100% germinal silanols. For α-cristobalite, the common (1 0 0) plane was covered by germinal silanols, whereas the (1 1 1) and (1 1 0) planes were covered by isolated silanols only. Unlike many brittle crystals, SiO_2 polymorphs typically reveal no perfect crystallographic planes of cleavage other than some dominant fracture planes. Multiple species and distributions of silanols on the dominant fracture planes of α-quartz and α-cristobalite may cause surface sites with different acidities and the observed heterogeneity in the pH response [28]. Fisk et al. [6] reported that two types of silanols on the surface of quartz exhibited different pK_a values, i.e., $pK_{Q3} = 4.5$ (more acidic), and $pK_{Q2} = 8.5$ (less acidic). The different relative proportions of the two silanols resulted in the heterogeneity of the surface acidity between α-quartz and α-cristobalite. Moreover, according to our present results, the surface site density of α-quartz was higher than that of α-cristobalite. Hence, it could be deduced that a much greater quantity of isolated silanols existed on the surface of α-quartz. This conclusion was consistent with the previous findings obtained using the model calculation [14].

3.4. Effect of SSA

SiO_2 polymorphs are tectosilicate minerals without porous and open structures. Clearly, surface silanols are dominantly responsible for the reactivity of silica. Consequently, the SSA plays a key role in the physical and chemistry interface reaction processes. The amount of MB adsorbed on α-quartz and α-cristobalite positively correlated with their SSA (Fig. 5) Interestingly, even though both were composed of silica, the linear relationship between the amount of adsorbed MB and the SSA in α-quartz was inconsistent with that of α-cristobalite. The relationship was well described by two lines with different slopes (Fig. 5) It could be concluded that the surface heterogeneities of α-quartz and α-cristobalite were not fully controlled by their SSA, and the difference in surface microstructures and properties exerted a significant effect. The influence of SSA on CV adsorption on the α-quartz and α-cristobalite followed the same pattern (Fig. 5 insert).

3.5. Effect of initial pH

The solution pH is a critical factor affecting the adsorption characteristics of α-quartz and α-cristobalite. The adsorption amount of MB on α-quartz and α-cristobalite rapidly increased with increasing pH until 3.0, after which both increased more slowly (Fig. 6). The adsorption isotherms of MB on α-quartz and α-cristobalite at different pH values (pH 3, 5, 8) at 28 °C were all best fit with

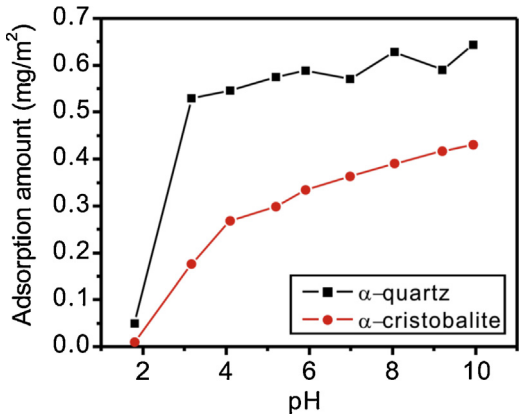

Fig. 6. Adsorption amount of MB on α-quartz and α-cristobalite as a function of initial pH.

the Langmuir adsorption model, which were depicted in Fig. 7 The isotherms clearly showed that the adsorption capacity of MB on α-quartz varied little with the pH increased from 3 to 8, ranging from 0.70 mg/m^2 to 0.78 mg/m^2. In line with α-quartz, the saturated adsorption amount of α-cristobalite increased from 0.20 mg/m^2 to 0.37 mg/m^2 with the pH increased from 3 to 8.

It is well known that silanol groups (Si—OH) naturally exist on the surface of silica minerals [16,29]. According to the plot of the zeta potential as a function of pH, the pH_{PZC} of α-quartz and α-cristobalite were 2.8 and 3.2, respectively. Generally, when the solution pH was higher than the pH_{PZC}, Si—O$^-$ sites could be produced because of deprotonation reaction, seen in reaction (3) [30]. Under this pH condition, MB was positively charged and served as MB$^+$. Hence, MB$^+$ could be adsorbed on the negative surface via electrostatic attraction, as depicted in reaction (4). Furthermore, the electrostatic interaction between MB$^+$ and Si—O$^-$ was absolutely dominant during the adsorption of MB onto α-quartz and α-cristobalite. With the pH increase, more deprotonation resulted in a larger amount of Si—O$^-$ on the surface [31]. Consequently, a higher adsorption capacity of MB on α-quartz and α-cristobalite was obtained.

$$> \text{Si—OH} + \text{OH}^- \Rightarrow \text{Si—O}^- + \text{H}_2\text{O} \quad (3)$$

$$> \text{Si—O}^- + \text{M}^+ \Rightarrow \text{Si—O—M} \quad (4)$$

Considering the results of surface site titration, the surface site density of α-quartz was higher than that of α-cristobalite; correspondingly, the amount of adsorbed MB on α-quartz was larger than that on α-cristobalite at an identical pH. Meanwhile, the drastic increase in the adsorption capacity of MB on α-quartz caused by raising the pH from approximately 2 to 3 (Fig. 6) should not be exclusively because the adsorption amount did not change much when the pH was increased to values greater than 3, and the same effect occurred in α-cristobalite. It is known that there are two silanol species (isolated and germinal) with different pK_a values [32] on the surface of α-quartz and α-cristobalite. At a low pH, the adsorption was dominated by the deprotonated Q^3 sites, whereas Q^2 and Q^3 site binding would prevail on the sample surface at a higher pH. Compared with α-cristobalite, the amount of isolated silanols (Q^3 sites) on α-quartz was larger, considering the previous theoretical research [10]. Therefore, the larger amount of isolated silanols on α-quartz accounted for the drastic increase in the adsorption amount that accompanied the pH increased from 2 to 3. To be specific, when the solution pH was lower than 3, the isolated silanols with lower pK_a values could more easily complete the deprotonation reaction with the increasing pH, and produce more Si—O$^-$ sites on the surface. By contrast, at higher pH values, the deprotonation and adsorption reactions in α-quartz occurred relatively gradually. That could be accounted for that the total quantity of silanols (isolated and germinal) on α-quartz was larger than that on α-cristobalite.

3.6. Thermodynamics study

The adsorption capacity of MB on α-quartz and α-cristobalite was favored by elevating the temperature (Fig. 8) The thermodynamic parameters, including the Gibbs free energy (ΔG), enthalpy (ΔH) and entropy (ΔS), could be obtained from the experiments at various temperatures by the following equations: [33]

$$\Delta G = -RT \ln K \quad (5)$$

$$\ln K = \frac{\Delta S}{R} - \frac{\Delta H}{RT} \quad (6)$$

where R is the gas constant (8.3145 J mol^{-1} K^{-1}) and T is the absolute temperature in Kelvins (K). K is the distribution coefficient for adsorption determined as:

$$K = \frac{q_e \frac{m}{v}}{C_e} \quad (7)$$

where q_e is the amount of MB adsorbed on the adsorbents at equilibrium (mg/g), C_e is the equilibrium concentration of MB in solution (mg/L), m is the mass of adsorbent (g), and v is the volume of the MB solution (L). ΔH and ΔS could be calculated from the slope and intercept of the Van't Hoff plots of $\ln K$ versus $-1/T$. The values of ΔG were negative, which indicated that the adsorption of

Table 3
Thermodynamic parameters for the adsorption of MB onto α-quartz and α-cristobalite.

	ΔG (kJ/mol)			ΔH (kJ/mol)	ΔS (J/mol K)
	288 K	298 K	303 K		
α-Quartz	−1.37	−1.64	−2.41	16.71	62.47
α-Cristobalite	−2.41	−2.59	−3.14	10.31	43.93

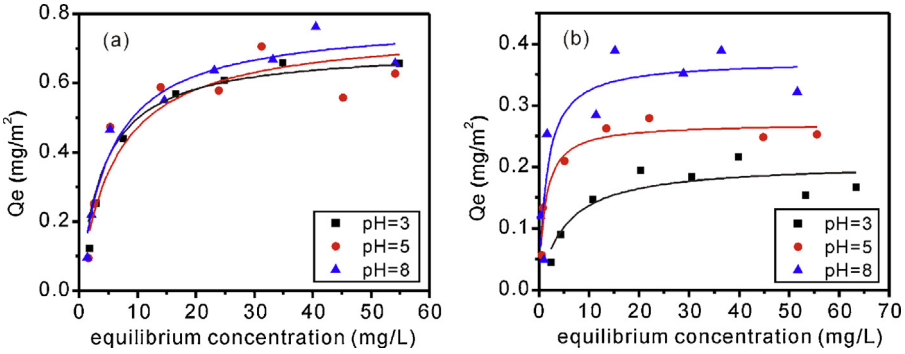

Fig. 7. Effect of different initial pH values on the adsorption of MB onto α-quartz (a) and α-cristobalite (b).

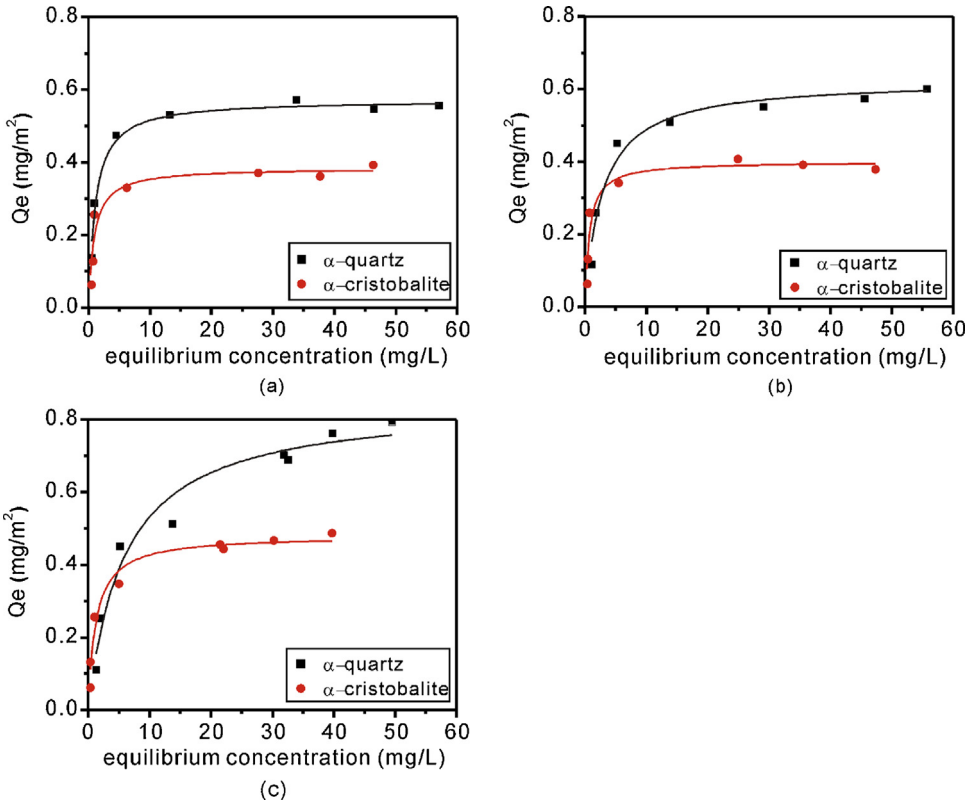

Fig. 8. Adsorption isotherms of MB onto α-quartz and α-cristobalite at 288 K (a), 298 K (b) and 303 K (c).

MB on both α-quartz and α-cristobalite was favorable and spontaneous (Table 3). The ΔH values were positive for the MB adsorption, corresponding to endothermic processes. The higher value of ΔH for α-quartz (16.71 kJ/mol) implied a much different adsorption behavior and spatial arrangement of MB on the surface, [13] compared with α-cristobalite (10.31 kJ/mol). The positive ΔS values reflected an increase in the randomness at the solid/solution interface, implying more possible arrangements during the adsorption of MB [34].

Additionally, according to our previous research, the surface site density of α-quartz and α-cristobalite controlled the spatial arrangement of MB adsorbed on the surface. In detail, the MB

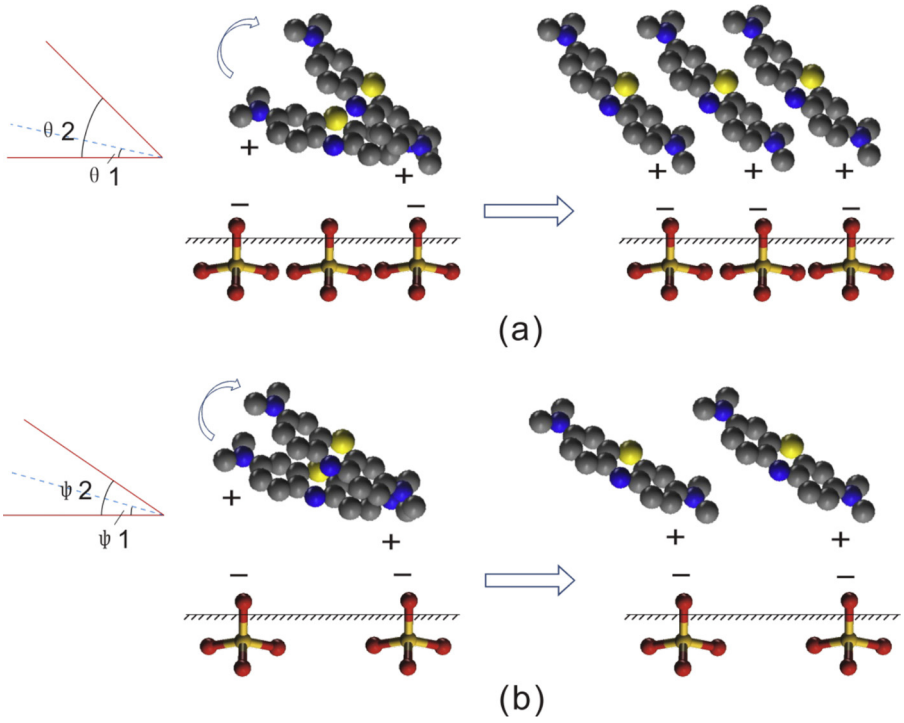

Fig. 9. Changes of the average tilt angle of the MB monomers on α-quartz (a) and α-cristobalite (b).

monomer went through from a lower tilt angle between the long axis of MB monomers and the sample surface to a larger one during the adsorption [13]. As shown in Fig. 9 α-quartz exhibited a larger angle change than α-cristobalite when the adsorption changed from the unsaturated state to the saturated. The higher value of ΔH for α-quartz could be used to account for its tilt angle change: more energy was needed to lift the free end of the MB monomer, thereby elevating the average tilt angle. The different thermal effects were also good indicators of the various adsorption behaviors of α-quartz and α-cristobalite caused by their surface heterogeneities.

4. Conclusions

The surface site titration results along with Gran plots showed that the surface site density of α-quartz was higher than that of α-cristobalite. Furthermore, compared with α-cristobalite, the pH_{PZC} of α-quartz was much lower, suggesting that the capacity of proton-donating by α-quartz was stronger than that by α-cristobalite. As a consequence, the adsorption capacity of MB on α-quartz was larger than that on α-cristobalite under an identical condition. The adsorption amount of MB on α-quartz and α-cristobalite were both positively related with their SSA. The equilibrium data were well described by the Langmuir isotherm model, indicating that the adsorption occurred on a homogeneous surface by monolayer sorption. The amount of MB adsorbed on both α-quartz and α-cristobalite increased with the increased initial pH, whereas, the deprotonation and adsorption reactions occurred dramatically on α-quartz at a lower pH owing to its larger quantity of isolated silanols. Combined with the characteristics of MB and the two minerals surface, it could be inferred that the adsorption involved electrostatic attraction and competition with the protons for the cationic sites. Furthermore, the thermodynamic parameters indicated the adsorption of MB was spontaneous and endothermic. The adsorption processes of MB on α-quartz and α-cristobalite were favored by increasing the temperature. From the perspective of molecule topology, the higher ΔH value of α-quartz (16.71 kJ/mol) implied a larger average tilt angle change of MB monomers on its surface.

The topic of this study was focused on a comparison of surface chemistry and reactivity of α-quartz and α-cristobalite. As one of the most abundant mineral species in the soil and sediments, the heterogeneity will play a significant role in the environmental remediation. The results of this study give a good baseline for the importance of surface properties which SiO_2 polymorph minerals performed in environmental evaluation and industrial applications.

Acknowledgements

This work was supported by CAS/SAFEA International Partnership Program for Creative Research Teams (Grant 20140491534) and National Natural Science Foundation of China (Grants U1201233, 41073084).

Appendix A. Supplementary data

Supplementary data associated with this article can be found, in the online version, at http://dx.doi.org/10.1016/j.apsusc.2015.07.214

References

[1] Y.S. Zeng, Y. Yang, Experimental study about gold deposition on the quartz surface, Geol. Rev. 41 (1995) 277–282.
[2] S. Sjoberg, Silica in aqueous environments, J. Non-Cryst. Solids 196 (1996) 51–57.
[3] Y.E. Freedman, M. Magaritz, G.L. Long, D. Ronen, Interaction of metal with mineral surfaces in a natural groundwater environment, Chem. Geol. 116 (1994) 111–121.
[4] C.J. Horwell, B.J. Williamson, K. Donaldson, J.S. Le Blond, D.E. Damby, L. Bowen, The structure of volcanic cristobalite in relation to its toxicity; relevance for the variable crystalline silica hazard, Part. Fibre Toxicol. 9 (2012) 44.
[5] B. Fubini, Surface chemistry and quartz hazard, Ann. Occup. Hyg. 42 (1998) 521–530.
[6] J.D. Fisk, R. Batten, G. Jones, J.P. O'Reilly, A.M. Shaw, pH dependence of the crystal violet adsorption isotherm at the silica–water interface, J. Phys. Chem. B 109 (2005) 14475–14480.
[7] C. Leodopoulos, D. Doulia, K. Gimouhopoulos, Adsorption of cationic dyes onto bentonite, Sep. Purif. Rev. 44 (2014) 74–107.
[8] E. Eren, B. Afsin, Investigation of a basic dye adsorption from aqueous solution onto raw and pre-treated sepiolite surfaces, Dyes Pigm. 73 (2007) 162–167.
[9] G.O. El-Sayed, Removal of methylene blue and crystal violet from aqueous solutions by palm kernel fiber, Desalination 272 (2011) 225–232.
[10] C.M. Koretsky, D.A. Sverjensky, N. Sahai, A model of surface site types on oxide and silicate minerals based on crystal chemistry; implications for site types and densities, multi-site adsorption, surface infrared spectroscopy, and dissolution kinetics, Am. J. Sci. 298 (1998) 349–438.
[11] V. Murashov, M. Harper, E. Demchuk, Impact of silanol surface density on the toxicity of silica aerosols measured by erythrocyte haemolysis, J. Occup. Environ. Hyg. 3 (2006) 718–723.
[12] A.S. Gibson, J.P. LaFemina, Structure of mineral surface, in: P.V. Brady (Ed.), Physical and Chemistry of Mineral Surface, CRC Press Inc., USA, 1996, pp. 1–62.
[13] C.H. Tang, J.X. Zhu, Q. Zhou, J.M. Wei, R.L. Zhu, H.H. He, Surface heterogeneity of SiO_2 polymorphs: an XPS investigation of α-quartz and α-cristobalite, J. Phys. Chem. C 118 (2014) 26249–26257.
[14] V.V. Murashov, E. Demchuk, Surface sites and unrelaxed surface energies of tetrahedral silica polymorphs and silicate, Surf. Sci. 595 (2005) 6–19.
[15] A. Legrand, H. Taïbi, H. Hommel, P. Tougne, S. Leonardelli, Silicon functionality distribution on the surface of amorphous silicas by ^{29}Si solid state NMR, J. Non-Cryst. Solids 155 (1993) 122–130.
[16] P. Yuan, D.Q. Wu, Z. Chen, Z.W. Chen, Z.Y. Lin, G.Y. Diao, J.L. Peng, ^{1}H MAS NMR spectra of hydroxyl species on diatomite surface, Chin. Sci. Bull. 46 (2001) 1112–1115.
[17] F. Musso, M. Sodupe, M. Corno, P. Ugliengo, H-bond features of fully hydroxylated surfaces of crystalline silica polymorphs: a periodic B3LYP study, J. Phys. Chem. C 113 (2009) 17876–17884.
[18] V. Bolis, B. Fubini, S. Coluccia, E. Mostacci, Surface hydration of crystalline and amorphous silicas, J. Therm. Anal. 30 (1985) 1283–1292.
[19] V. Bolis, B. Fubini, E. Giamello, Effect of form on the surface chemistry of finely divided solids, Mater. Chem. Phys. 29 (1991) 153–164.
[20] B. Fubini, V. Bolis, A. Cavenago, E. Garrone, P. Ugliengo, Structural and induced heterogeneity at the surface of some SiO_2 polymorphs from the enthalpy of adsorption of various molecules, Langmuir 9 (1993) 2712–2720.
[21] V. Bolis, A. Cavenago, B. Fubini, Surface heterogeneity on hydrophilic and hydrophobic silicas: water and alcohols as probes for H-bonding and dispersion forces, Langmuir 13 (1997) 895–902.
[22] H.H. Wu, D.Q. Wu, Study on surface site types of quartz and calcium carbonate by FDIR spectroscopy, J. Mineral. Petrol. 19 (1999) 1–4.
[23] G. Gran, Determination of the equivalence point in potentiometric titrations. Part II, Analyst 77 (1952) 661–671.
[24] Q. Du, Z.X. Sun, W. Forsling, H.X. Tang, Acid–base properties of aqueous illite surfaces, J. Colloid Interface Sci. 187 (1997) 221–231.
[25] W.M. Zhang, Z.D. Yang, J. Liu, Z.X. Sun, Determination of acid–base equilibrium constants on aqueous mesoporous silica surface, Acta Phys. Chim. Sin. 26 (2010) 2109–2114.
[26] D.E. Yates, F. Grieser, R. Cooper, T.W. Healy, Tritium exchange studies on metal-oxide colloidal dispersions, Aust. J. Chem. 30 (1977) 1655–1660.
[27] A.C. Riese, Adsorption of Radium and Thorium onto Quartz and Kaolinite: A Comparison of Solution/Surface Equilibria Models, Colorado School of Mines, 1982.
[28] S. Kasar, S. Kumar, A.S. Kar, S.V. Godbole, B.S. Tomar, Sorption of Eu(III) by amorphous titania, anatase and rutile: denticity difference in surface complexes, Colloids Surf. A 434 (2013) 72–77.
[29] P.V. Brady, The Physics and Chemistry of Mineral Surfaces, CRC Press, 1996.
[30] O.S. Pokrovsky, S.V. Golubev, J.A. Mielczarski, Kinetic evidences of the existence of positively charged species at the quartz–aqueous solution interface, J. Colloid Interface Sci. 296 (2006) 189–194.
[31] J. Zhang, D.Q. Cai, G.L. Zhang, C.J. Cai, C.L. Zhang, G.N. Qiu, K. Zheng, Z.Y. Wu, Adsorption of methylene blue from aqueous solution onto multiporous palygorskite modified by ion beam bombardment: effect of contact time, temperature, pH and ionic strength, Appl. Clay Sci. 83–84 (2013) 137–143.
[32] S.W. Ong, X.L. Zhao, K.B. Eisenthal, Polarization of water-molecules at a charged interface – second harmonic studies of the silica water interface, Chem. Phys. Lett. 191 (1992) 327–335.
[33] M. Eloussaief, I. Jarraya, M. Benzina, Adsorption of copper ions on two clays from Tunisia: pH and temperature effects, Appl. Clay Sci. 46 (2009) 409–413.
[34] L.Y. Zhang, H.Y. Zhang, W. Guo, Y.L. Tian, Removal of malachite green and crystal violet cationic dyes from aqueous solution using activated sintering process red mud, Appl. Clay Sci. 93–94 (2014) 85–93.